Received: 20 October 2021 | Revised: 2 May 2022 | Accepted: 5 May 2022 | Published on: 7 June 2022

DOI: 10.1002/joc.7700

RESEARCH ARTICLE

International Journal of Climatology RMetS

Long-term evolution of cold air pools over the Madrid basin

Domingo F. Rasilla[1] | **Alberto Martilli**[2] | **Fernando Allende**[3] | **Felipe Fernández**[3]

[1]Departamento de Geografía, Urbanismo y Ordeanción del Territorio, Universidad de Cantabria, Santander, Spain

[2]División de Contaminación Atmosférica, Centro Investigaciones Energéticas, Medioambientales y Tecnológicas, Madrid, Spain

[3]Departamento de Geografía, Universidad Autónoma de Madrid, Madrid, Spain

Correspondence

Domingo F. Rasilla, Departamento de Geografía, Urbanismo y Ordeanción del Territorio, Universidad de Cantabria, 39005 Santander, Spain.

Email: domingo.rasilla@unican.es

Funding information

Secretaría de Estado de Investigación, Desarrollo e Innovación, Grant/Award Number: CGL2016-80154-R

Abstract

Cold air pools (CAPs) are one of the most severe weather conditions experienced across many basins worldwide, related to episodes of extreme cold temperatures, poor air quality, and disruption of transportation networks. This study offers a basic climatology of CAPs in the southern Spanish Plateau and investigates its evolution since 1961 and their links with local, synoptic, and large-scale climate variability. It is based on the comparison of meteorological records from two stations, one in the Sistema Central Range (Navacerrada, 1,894 m asl) and another at the plain (Madrid-Barajas, 609 m asl). Accuracy and representativeness of both locations to depict the spatial and temporal variability of CAPs was also tested. CAPs days (defined as the simultaneous occurrence of a daily minimum temperature difference above 0.1°C between both stations) were found to occur year-round, but the most frequent and intense occur in winter (NDJ). Some typical features of CAPs, such as local mesoscale processes (katabatic and anabatic flows) in connection with synoptic (advection of mid-troposphere warm air masses during high-pressure regimes) and hemispheric (a positive phase of the North Atlantic Oscillation) variability were also observed, leading to a sheltered boundary layer at the bottom of southern Spanish Plateau, decoupled from the free troposphere. By night, CAPs have maintained both their frequency and intensity, which means that the frequency of extremely cold nights on the plain has remained relatively stable (despite global warming). By day, an enhanced warming of the high-elevation site has increased the temperature difference between the mountains and the plain during CAP days.

KEYWORDS

cold air pools, North Atlantic Oscillation, Madrid Basin (Spain)

1 | INTRODUCTION

Cold air pools (henceforth CAP) make up one of the most singular disturbances exerted by the terrain upon the vertical and horizontal temperature fields. Essentially, a CAP can be defined as a topographically confined, stagnant layer of air colder than the air above (Whiteman, 2000; Barry, 2008). Several mechanisms at different scales interact in its genesis, evolution, and break up. Its simplest version results from a bottom-up cooling: during clear and calm nights the loss of long-wave radiation and the lack of turbulence cools the air in contact with the earth's surface at the bottom of small depressions (sinkholes, poljes, etc.), sheltered by the surrounding topography (Price *et al.*, 2011; Sheridan *et al.*, 2014). In larger landforms (valleys, basins, or plateaus) those cooled air masses will drain from the higher ground through thermally driven circulations which eventually will also become trapped (Schmidli *et al.*, 2009; Zardi and Whiteman, 2013; Burns and Chemel, 2014). The overlapping of a surface cold air mass by a warmer air mass reverts the typical vertical temperature gradient within the planetary boundary layer, creating a temperature inversion. Although most of these nocturnal accumulations disappear the following morning, this cycle of nocturnal genesis and diurnal break-up can repeat over several days, persisting occasionally even during daytime hours.

CAPs also disrupt other atmospheric variables. A boundary layer less ventilated accumulates pollutants close to their sources; when those conditions persist for days, pollutants very often exceed threshold values imposed by national/international directives (Silcox *et al.*, 2012; Whiteman *et al.*, 2014; Green *et al.*, 2015; Largeron and Staquet, 2016b; Ivey *et al.*, 2019). The worsening of the air quality triggers serious health problems (Palmieri *et al.*, 2008; Beard *et al.*, 2012) and forces action protocols regulating the public access to the specific neighbourhoods (Holman *et al.*, 2015; Borge *et al.*, 2018; Romero *et al.*, 2019; Salas *et al.*, 2021). Additionally, increases of relative humidity as temperature falls below the dew point form layers of low strata or fog, reducing the visibility and disrupting transportation (Hodges and Pu, 2016; Chachere and Pu, 2019). In valleys where CAPs occur frequently, they even control the spatial distribution and growth rates of vegetation (Blennow and Lindkvist, 2000; Dobrowski, 2011) and can constitute a risk factor in agricultural areas (Espín Sánchez, 2015).

Such singularities and dire impacts have supported a great bulk of research about CAPs in different regions of the globe following multiple approaches (e.g., Pyrenees: Miró *et al.*, 2018; Pagès *et al.*, 2017, Alps: Zängl, 2005a, Zängl, 2005b; Chemel *et al.*, 2016; Hiebl and Schöner, 2018, Carpathians: Bărcăcianu and Apostol, 2014, western United States: Daly *et al.*, 2009; Whiteman *et al.*, 2001; Lu and Zhong, 2014, or Chile: Gramsch *et al.*, 2014). Pseudo vertical temperature gradients have been evaluated from ground-based meteorological networks, either from permanent observatories (Pepin, 2001; Rolland, 2003; Kirchner *et al.*, 2013; Largeron and Staquet, 2016a; Navarro-Serrano *et al.*, 2018; Joly and Richard, 2019; Kikaj *et al.*, 2019) or temporary networks installed ad hoc during experimental campaigns (Whiteman *et al.*, 2004; Steinacker *et al.*, 2007; Miró *et al.*, 2018). Variability of the vertical structure of the atmosphere during CAPs has been also studied using radiosondes, tethered balloons, SODAR, or airplanes (Wolyn and Mckee, 1989; Clements *et al.*, 2003; Yao and Zhong, 2009; Lareau *et al.*, 2013; Lehner *et al.*, 2015; McCaffrey *et al.*, 2019). The dynamics of those events have been simulated through mesoscale models (Largeron and Staquet, 2016b; Lehner *et al.*, 2017; Pagès *et al.*, 2017; Flores *et al.*, 2020). Topics have focused on physical processes such as inversion build-up and rupture, wind systems (Steinacker *et al.*, 2007; Leukauf *et al.*, 2015), environmental impacts (Schnitzhofer *et al.*, 2009; Curtis *et al.*, 2014; Chemel and Burns, 2015), as well as their connections with synoptic or large-scale circulation patterns (Gillies *et al.*, 2010a; 2010b; Wang *et al.*, 2012; 2013; Wang *et al.*, 2015). Much less is known about the temporal evolution of the frequency and magnitude of CAPs over longer periods of time (Bailey *et al.*, 2011; Tingting *et al.*, 2021), due usually to the lack of proper long-term homogeneous meteorological time series. Only recently, such drawback is being overcome using long-term, high-resolution reanalysis datasets (Yu *et al.*, 2017; Palarz *et al.*, 2019; Palarz *et al.*, 2020).

Because of its significant impacts and challenges to numerical modelling and forecasting, analysis on CAP climatological characteristics and dynamics are highly relevant for human activities and the environment, which, in turn, it should direct us to assess the possible impacts of these episodes and the development of long-term planning and mitigation strategies for the future. Urban areas offer a suitable environment to look at CAP events and their consequences in terms of human comfort and air quality issues. Therefore, our objective has been to provide a basic characterization of CAPs and an assessment of their temporal trends at a sector of the southern Spanish Plateau, around the city of Madrid, an area which is populated by more than 6 million people, affected recurrently by episodes of adverse air quality. To do this, we have organized our work on four steps:

1. To assess the suitability of two meteorological observatories as representatives of the frequency and strength of CAPs in the study region.
2. To characterize the seasonal and interannual variability of CAPs and to quantify changes in frequency and intensity over the last 60 years.
3. To identify the synoptic background that induce the formation of CAP and to examine their connections with the interannual and decadal variability of large-scale circulation indices.
4. To document the relationship between those features and the recent regional climate evolution in the context of ongoing global warming.

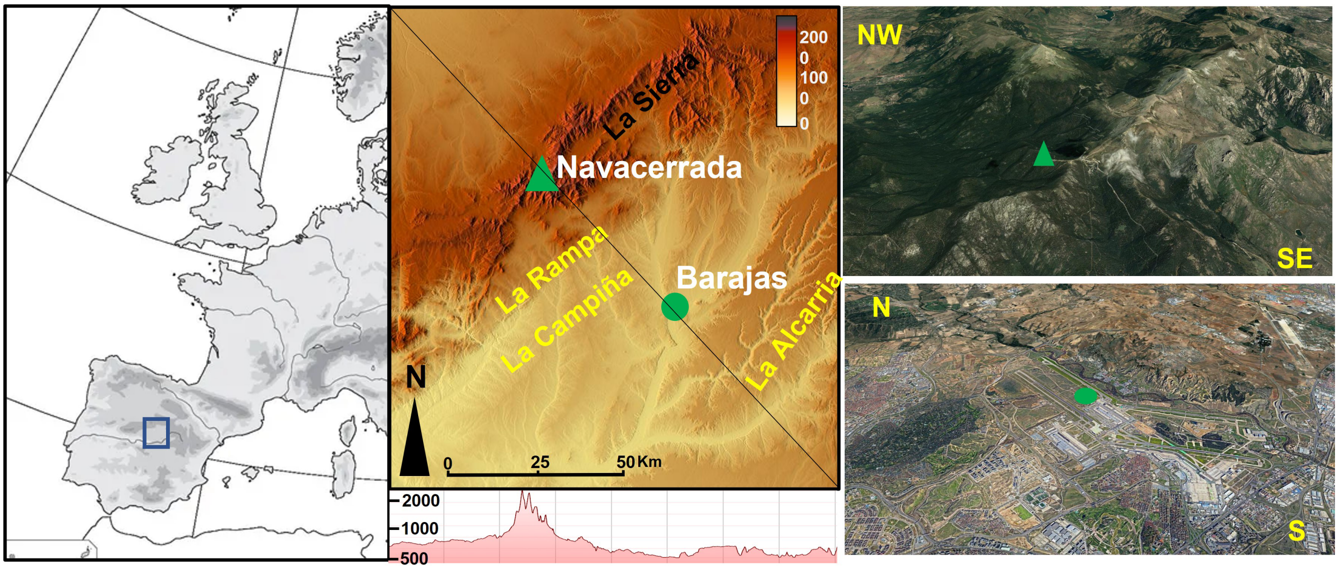

FIGURE 1 Study region, topographic map with the locations (green triangle, mountain station; circle, plain station) and aerial view of the surroundings of the basic meteorological stations. *Source*: Google Earth [Colour figure can be viewed at wileyonlinelibrary.com]

2 | STUDY AREA, DATA SOURCES, AND METHODOLOGY

2.1 | Study area

The study area is located at the centre of the Iberian Peninsula (Figure 1). Three different physiographic units are distinguished from north to south: the mountains (La Sierra), the piedmont (La Rampa), and the plains (La Campiña). The mountains run from SW to NE, reaching a maximum height of 2,440 m asl. The piedmont is a gradually sloping ramp, whose altitude progressively descends from 1,000 m to 800 m. The plains are made up of elongated and narrow hills, separating wide river meadows, mostly oriented from NW-N to SE-S. Its altitude descends from 800 to 500 m, ending at the course of the Tagus River. A mesa-like landscape (La Alcarria) appears at the SE corner, whose flat tops reach up to 1,000 m.

According to the Köppen–Geiger classification (Kottek *et al.*, 2006), the regional climate is Mediterranean, bordering the semi-arid class (Csa – BSk) in the plain, much wetter and cooler at the mountains.

2.2 | Meteorological data

The basic data of our analysis are the daily maximum and minimum temperature time series from Navacerrada (at 1,894 m asl) and Alfonso-Suarez Barajas-Airport (henceforth Barajas, 609 m asl), complemented by time series of daily averages of wind speed, relative air humidity and total sunshine hours. Those series, spanning from 1961 to 2020 and provided by the Spanish Meteorological Agency (AeMet), are almost complete. Navacerrada record is homogeneous, but temperature from Barajas show an inhomogeneity prior to 1962. Correction factors were calculated from the comparison of a monthly longer time series (1945–2020) with nearby stations, following the method proposed by Alexandersson (1986). Additionally, a shorter (2012–2016) database consisting of hourly temperature, relative humidity, and wind speed records from Navacerrada and Barajas, and daily minimum temperatures corresponding to other 24 meteorological stations scattered through the study area were also provided by AeMet.

NCEP/NCAR Reanalysis data for the period 1961–2020 was used to identify the most favourable atmospheric circulation features associated with CAP occurrence (Kalnay *et al.*, 1996). Composites of several surface, low- and mid-tropospheric meteorological variables were extracted through the web site application (https://psl.noaa.gov/data/composites/day/).

Seasonal indices of major teleconnection patterns were downloaded from the Climate Prediction Center web site (https://www.cpc.ncep.noaa.gov/data/teledoc/telecontents.shtml). Additionally, indices quantifying the strength and location of the Azores High were obtained from the Centers of Action web page at Stony Brook University (https://you.stonybrook.edu/coaindices/). The original monthly values of those large-scale indices were averaged into seasonal averages.

2.3 | Methodology

To date most climatological studies of CAPs have relied primarily on the comparison of temperature records from stations located at different altitudes, complemented by the analysis of low troposphere sounding records. Although a significant progress in homogenization of sounding temperature data have been achieved, their use for long-term analysis of CAPs is still hindered by discontinuities, resulting from changes of equipment, and observing practices (Dai *et al.*, 2011; Haimberger 2007; Durre *et al.*, 2018). On the other side, a correct evaluation of vertical changes in air temperature should require a dense network of devices to ensure the horizontal homogeneity of temperature fields, since pseudo-vertical temperature gradients extracted from ground surface stations can be distorted by mesoscale processes such as local drainage flows, night jets or localized turbulence (Whiteman *et al.*, 2004; Williams *et al.*, 2013).

CAPs have been identified in this study through a statistical approach, from the assessment of a reliable database which allow to derive a metric that adequately represents the nature of CAPs, a threshold to account exceedances and indices depicting their frequency and strength. A CAP day was defined as a day when the difference in daily minimum temperature between Navacerrada and Barajas was greater than 0.1°C; a positive value means that Navacerrada is warmer than Barajas (thus a temperature inversion) while a negative value implies that Navacerrada is colder than Barajas (the climatological lapse rate). This arbitrary threshold was chosen for pragmatic reason as other more complicated approaches would be difficult to apply to this dataset and assures to identify the strongest events. In addition, the value of that difference in daily minimum temperature was also used as a proxi of the strength of a CAP.

However, the comparison between just two individual stations to identify and characterize CAPs in the Spanish Southern Plateau might induce misleading results, although the distance between them is only less than 50 km. Consequently, an assessment of the representativeness of Navacerrada and Barajas to mirror CAP dynamics over our study area was needed. That task was undertaken following early work by Lundquist and Cayan (2007) and Lundquist *et al.* (2008), which identified CAPs submitting daily minimum temperatures to an empirical orthogonal function (EOF) technique. Minimum temperatures were used because the end of the night is the moment with the strongest CAPs signal. This methodology entails a previous filtering of the original series to remove the variability associated with the local conditions of each observatory (altitude, exposure, etc.) and dynamic mechanisms with a frequency higher than the synoptic variability (e.g., the seasonal cycle). The minimum temperature at a location $T\left(\vec{x},t\right)$ can be disaggregated in the following components:

$$T\left(\vec{x},t\right)=\overline{T}\left(\vec{x}\right)+\overline{T}'(t)+\widetilde{T}\left(\vec{x},t\right)+\varepsilon, \tag{1}$$

in which $\overline{T}\left(\vec{x}\right)$ is the average temperature of each location (primarily an elevation effect), $\overline{T}'(t)$ is the time deviation from the mean of each day (contribution of the synoptic variability), $\widetilde{T}\left(\vec{x},t\right)$ is the local anomalies of each observatory and finally, ε represents the instrumental error. Subtracting $\overline{T}\left(\vec{x}\right)$ and $\overline{T}'(t)$ from the original time series $T\left(\vec{x},t\right)$ removes the regional average lapse rate and the region-wide positive or negative temperature anomalies due to variability in weather patterns and creates a new time series which is then decomposed into their principal spatial patterns of variability and their evolution through time by using empirical orthogonal functions.

The underlying spatial structure is represented by the loadings of each observatory, while its intensity and temporal variability can be quantified through the scores of the principal components. The relationship between the temperature anomalies with loadings and scores is derived from this equation:

$$\widetilde{T}(x,y,t)+\varepsilon=\sum_{k=1}^{N}\mathrm{PC}(t)\,\mathrm{EOF}(x,y), \tag{2}$$

where $\mathrm{PC}_{(t)}$ is the score matrix and $\mathrm{EOF}_{(x,y)}$ is the loadings matrix. Lundquist and Cayan (2007) suggested that the first component usually represents the variability associated with cold air pools and accumulates most of the variability, thus Equation (2) can be simplified as

$$\widetilde{T}(x,y,t)+\varepsilon\approx\mathrm{PC1}(t)\,\mathrm{EOF}(x,y), \tag{3}$$

where $\mathrm{PC1}_{(t)}$ represents the first principal component and $\mathrm{EOF}_{(x,y)}$ the first component.

Links between indices of frequency and strength of CAPs with local (wind speed, relative sunshine duration, relative air humidity, etc.) and regional climatic parameters (teleconnection patterns) were explored through correlation (Spearman correlation coefficient) analysis and graphical procedures. When suspicious of the influence of a third variable on the correlation outcome, partial correlations were used to control the effect of that variable (also known as "control" variable). Detection and estimation of trends in time series was accomplished through the non-parametric Mann–Kendall and Theil–Sen's methods (Sen, 1968; Kendall, 1975). The first test is applicable to the detection of a monotonic trend of a time series, while the second fits a linear model for the trend.

For the analysis of the role of CAPs on the occurrence of very cold nights, a conventional statistical criterion, the 5th percentile value of the daily minimum temperature distribution, was adopted for purposes of identifying those extreme conditions.

3 | RESULTS

3.1 | Suitability of Navacerrada and Barajas temperature records to depict CAPs in the southern Spanish Plateau

To provide an initial characterization of the minimum temperature field during CAPs, we averaged the daily values recorded at 24 meteorological stations during days meeting the criteria to define CAPs and plotted it versus their altitude. As expected, the temperature increases with elevation (Figure 2a), a pattern consistent with the occurrence of a temperature inversion, but the lapse rate is deeper from the lowest sites up to ~800–1,000 m asl, meanwhile is only slightly positive upwards; this level might be the average altitude of the top of a surface inversion. Local effects somehow disturb this general pattern, for example, at some enclosed mountain valleys (Rascafría, 1,159 m asl), where negative anomalies up to 6°C on average are observed. This is the typical behaviour of narrow valleys experiencing strong sheltering effects and low vertical air mixing (Sheridan *et al.*, 2014). Conversely, anomalous warmer values are found on some sites in the Rampa (Colmenar Viejo, 1,004 m asl).

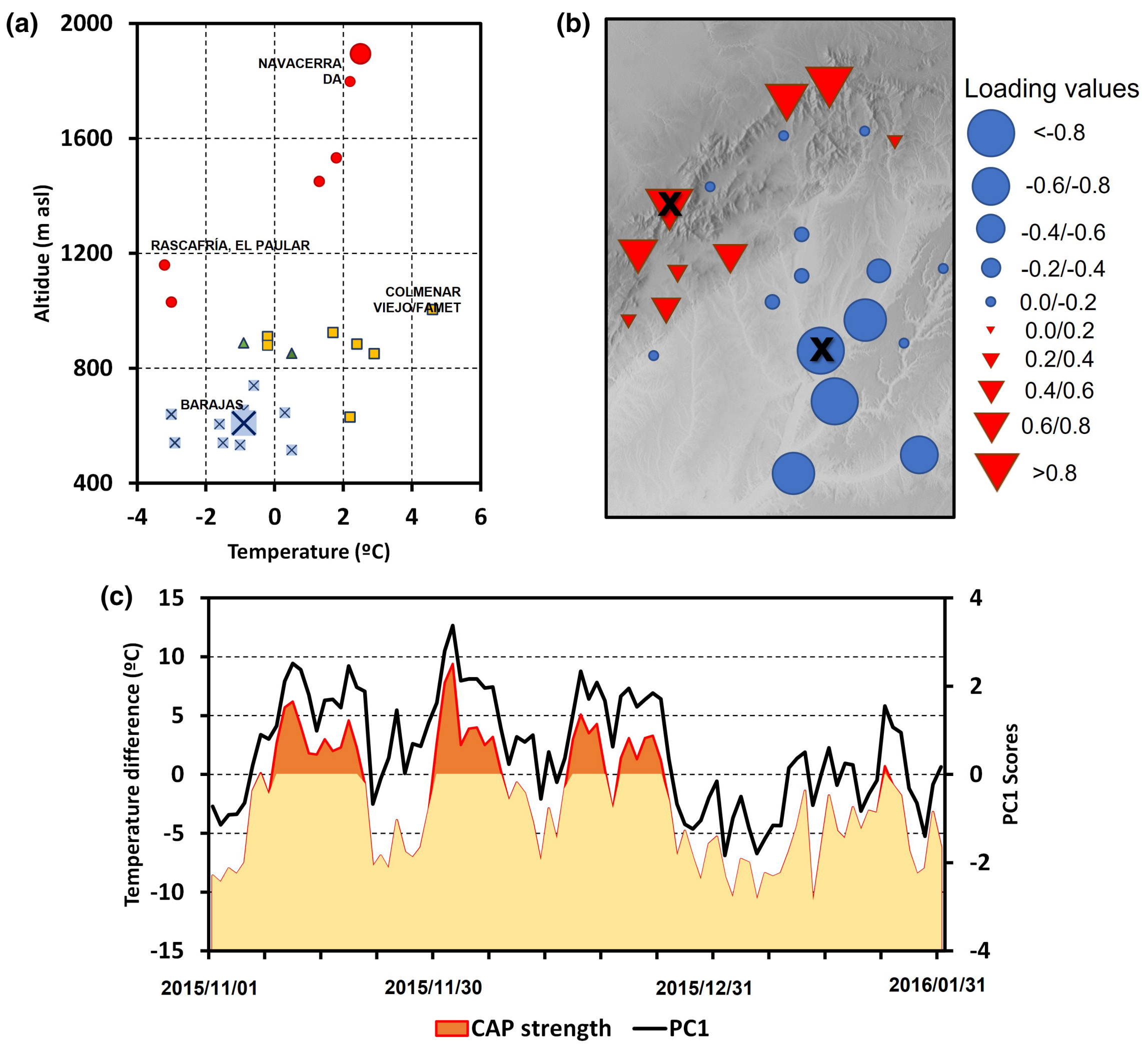

FIGURE 2 (a) Relationship between altitude and daily minimum temperatures during CAPs in the southern Spanish Meseta (2012–2016). Mountain stations are represented as red circles, piedmont stations as yellow squares, plain stations as blue squares and "Alcarria" stations as green triangles. (b) Spatial variation in EOF1 values representing CAP/no-CAP occurrence (X depicts Navacerrada and Barajas). (c) Temporal variation of PC1 (black line) and the difference between the minimum temperatures of Barajas and Navacerrada (red line) corresponding to the period November 1, 2015 to January 31, 2016. Orange colours correspond to CAP days [Colour figure can be viewed at wileyonlinelibrary.com]

Time series of daily minimum temperature anomalies from those meteorological stations across the study area were submitted to EOF analysis, using a correlation matrix as input. The first component PC1 represents 43% of the variance; the Spearman's correlation coefficient between the PC1 loadings and elevation at each station is 0.73, corresponding to an increase in temperature with altitude. As expected, PC1 can be considered an index for CAPs. Depending on the sign of the loadings, observatories can be classified as favourable/unfavourable (negative/positive loading) to cold air accumulations (Figure 2b). Positive loadings occur at sites in the Sierra or the Rampa; negative loadings appear around the bottom of the valleys (Henares, Jarama). Navacerrada owes the second most positive value (0.83), after Colmenar Viejo (0.88), while Barajas and Arganda del Rey tie in the lowest negative value (−0.8).

Another output of the EOF procedure is a time series of daily values of PC1. The evolution of these daily values over time provides a calendar of the occurrence and strength of a CAPs on a particular day: days with positive (negative) values correspond to CAP (non-CAP) days. As an example, the evolution of PC1 over a complete winter season, from November 1, 2015, to January 31, 2016, shows several CAP events (Figure 2c). The plot also includes the daily values of the difference in minimum temperatures between Navacerrada and Barajas, used in this paper as index of CAP occurrence and strength. Both time series display a close temporal evolution, displaying four periods of CAP conditions with different length and intensity. To check the reliability of the relationship of both indices across the year, correlations between both time series were calculated on a monthly base (do not shown). Values are quite homogeneous across the year, although the highest correlations occur during winter and the lowest in summer (0.89 in December versus 0.78 in July). According to this procedure, the daily variability of the minimum temperatures in Navacerrada and Barajas is representative of the general spatial and temporal behaviour of CAPs in the southern Spanish Plateau.

3.2 | Seasonal and interannual variability of CAPs and changes over the last 60 years

Over the last 60 years, CAPs occurred in 10.78% of the total number of days (Figure 3a). Approximately 50% of the days record a shallow inversion (less than 2°C); a maximum of 13.2°C was measured on November 27, 1979. Although they even appear during the warmest months, the longest (more than four consecutive days) and more intense concentrate between November and January, while weaker and shorter sequences are predominant from April to

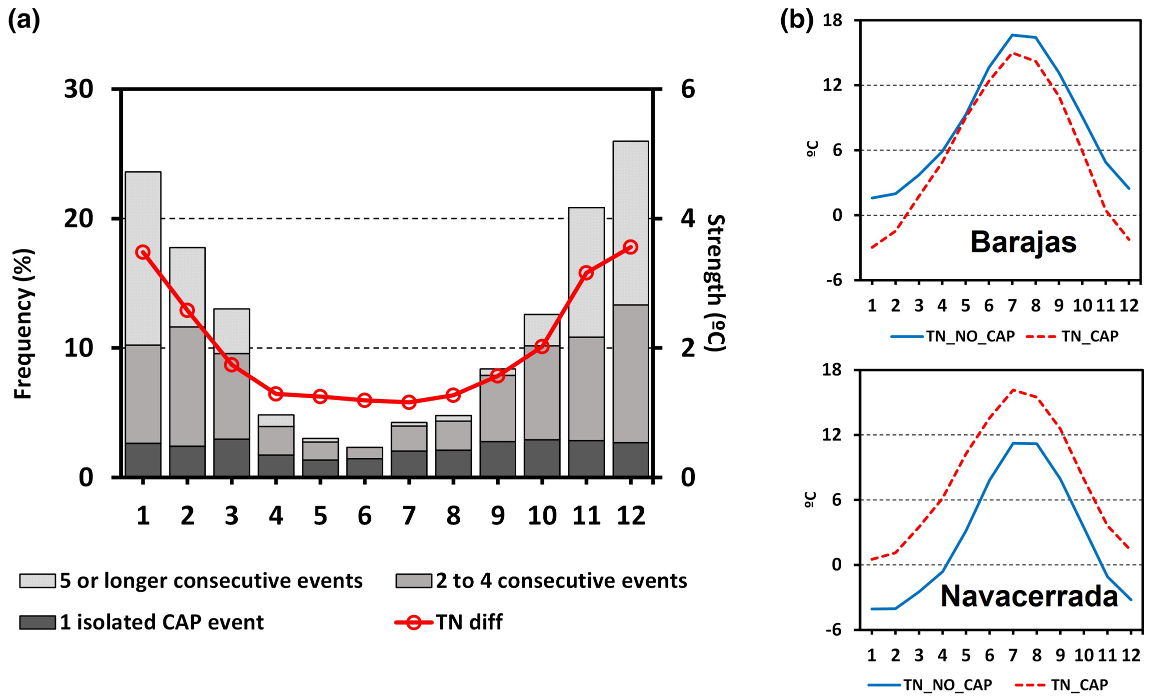

FIGURE 3 (a) Frequency (days) of CAPs according to the length of the sequences from 1961 to 2020. (b) Monthly average minimum temperatures at Navacerrada and Barajas during CAP (red line) and non-CAP days (blue line) from 1961 to 2020 [Colour figure can be viewed at wileyonlinelibrary.com]

September. When compared with no CAP conditions (Figure 3b), Barajas is always colder under CAPs, particularly from November to January (an average negative anomaly larger than 4°C) while Navacerrada is steadily warmer through the year (about 5.5°C). According to those features, we will focus on the November–January (NDJ) period for the rest of the paper.

Trends in the seasonal (NDJ) frequency and strength of CAPs during the 1961–2020 period were checked, but no significant trends were obtained. For sake of a better understanding of the dynamic mechanisms involved, we also submitted the seasonal averages of the difference in the maximum temperature on the same days to a trend analysis. A significant ($p < .05$) increase was obtained, related to a daytime warming trend at Navacerrada. (Figure 4 and Table 1).

The total NDJ frequency of CAP days were also correlated to its seasonal average strength (Spearman correlation coefficients $r = .44$, $p < .001$). At daily time scales, the correlation between duration (consecutive days) and strength (maximum temperature difference) of each episode confirms that the longer a CAP event persists, the more intense it is (Figure 5a), and such strengthening is largely the result of the warming of Navacerrada. However, this is only true for sequences shorter than 8–10 days; the relationship between both parameters follows a logarithmic model, in which the strength accelerates rapidly at first and then slows over time. Beyond that limit, atmospheric synoptic scale variability (most of the time the extreme tip of a cold front), although unable to destroy the CAP, usually alters the vertical stability of the regional atmosphere, through a cooling in Navacerrada and a higher day-to-day variability in Barajas (Figure 5b).

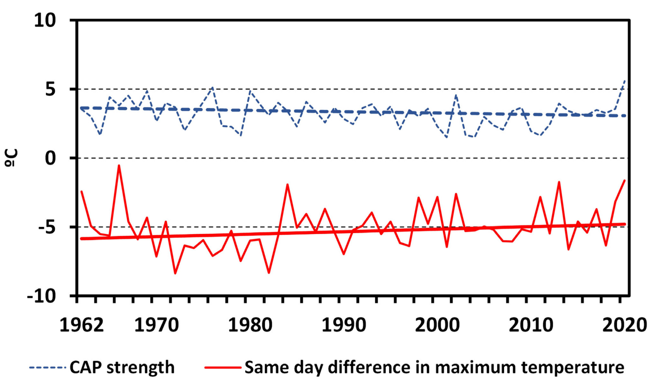

FIGURE 4 Long-term trends of CAP strength and same day difference in maximum temperature during winter (NDJ, 1961–2020) CAP days [Colour figure can be viewed at wileyonlinelibrary.com]

3.3 | Synoptic background and connections with large-scale circulation indices

This section is devoted to identifying and analysing the most favourable atmospheric circulation patterns for CAP days in the southern Spanish Plateau at two temporal and spatial time scales. First, composites of different upper air meteorological fields were assembled, consisting of arithmetic means obtained from a subsample of the original 0600 UTC values (the most probable hour of CAP occurrence) from the NCEP/NCAR Reanalysis data set. That subsample was based on the calendar of winter (NDJ 1961–2020) CAP days. A simultaneous representation of different atmospheric fields was provided, trying to make easier the interpretation the dynamic fields and the anomalous behaviour of the atmospheric circulation.

The composite of SLP (Figure 6a) shows strong anticyclone over the Iberian Peninsula, in fact an expansion of the Azores High towards the NE of its winter mid-position. Correspondingly, the SLP anomaly field

TABLE 1 *Z* statistic and significance (from a Mann–Kendall analysis), and slope (*Q*) and intercept (*β*) values (from a Theil–Sen analysis) applied to CAP frequency, CAP strength, same day difference in maximum temperature between Navacerrada and Barajas, and daily maximum and minimum temperature in Navacerrada and Barajas during winter (NDJ, 1961–2020) CAP days

	Z values	Significance	*Q* (slope)	*β* (intercept)
CAP frequency (days)	0.52		0.038	18.88
CAP strength (°C)	−1.34		−0.01	3.63
Same day difference in maximum temperature (°C)	1.96	+	0.027	−5.61
Tx_Navacerrada (°C)	2.94	**	0.44	68.27
Tn_Navacerrada (°C)	0.73		0.10	10.50
Tx_Barajas (°C)	1.46		0.18	126.94
Tn_Barajas (°C)	1.46		0.15	−22.90

Note: ** Trend at α = 0.01 level of significance. + Trend at α = 0.1 level of significance.

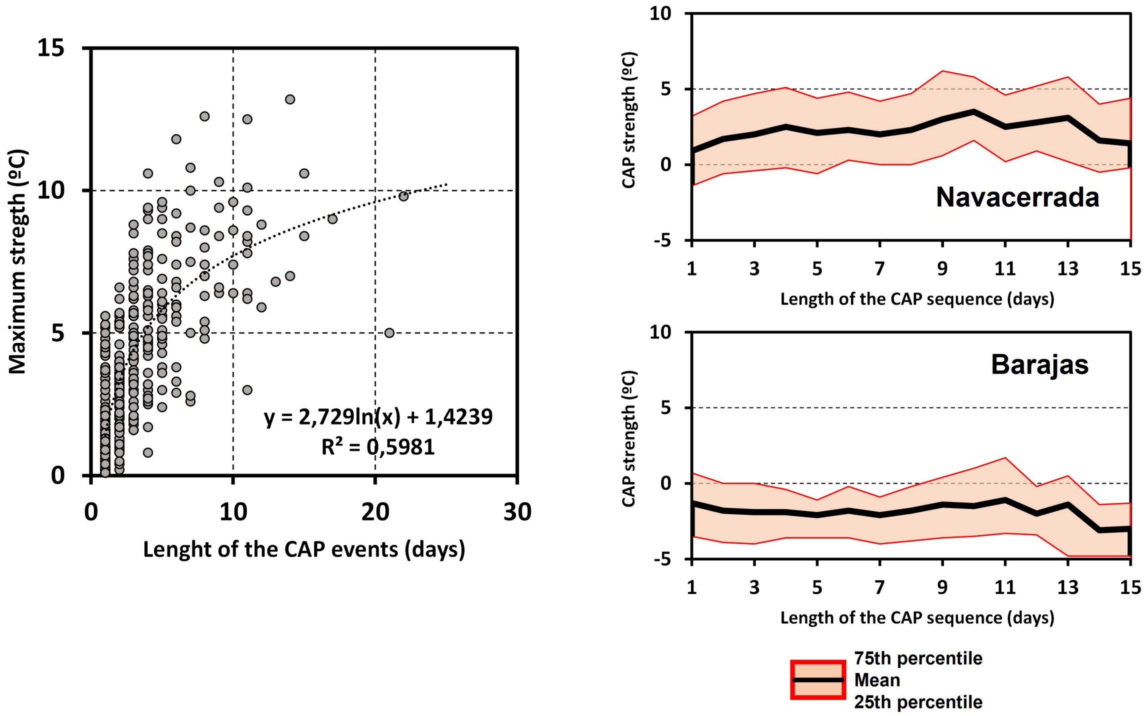

FIGURE 5 Relationship between the length of winter (NDJ, 1961–2020) CAP sequences (days) and maximum strength (maximum difference between daily minimum temperatures on each sequence, in °C) [Colour figure can be viewed at wileyonlinelibrary.com]

displays a strong positive anomaly centred around the Bay of Biscay, encompassing most of the Iberian Peninsula and Western Europe. Mid-tropospheric atmospheric circulation, represented by the 500 hPa height field (Figure 6b) is controlled by a strong ridge, whose main axis appears slightly displaced to Portugal. The corresponding anomaly field is characterized by a rather concentric positive anomaly centre located North of Iberia. Both synoptic features contribute to the anomalous warm and dry advection which seems to come from Northern Africa, as shown by the T850 and RH850 composite fields (Figure 6c,d, respectively). The composite for the 850 hPa wind field (Figure 6e) is generally in quite good geostrophic agreement with the SLP and Z500 composite fields, with regions of low or very low wind coinciding with the anticyclone/ridge and regions with closer isobars being characterized by moderate winds.

At a larger temporal and spatial scales, Table 2 shows the correlation between the seasonal frequency and average strength of CAPs with the corresponding values of the most relevant teleconnection patterns affecting Europa's climate. According to the results, only the frequency of CAP events was significantly correlated to the NAO and SCAND indices: high values of the NAO index correlate with high frequencies of CAPs (Figure 7), while a negative correlation was obtained for the SCAND index. However, when SCAND was submitted to a partial correlation analysis while holding NAO index as a fixed variable, correlation values become no significant. No significant correlation was found with other well-known mid-latitude teleconnection patterns.

To additionally assess if the relationship was sensitive not only to the phase of the NAO, but also to the strength and location of its southern node, the Azores High, a partial correlation coefficient between the CAP events and indices of strength and location with the effect of the NAO removed was calculated. No significant values were obtained either (not shown).

3.4 | Impacts on local winter climate variability

Table 3 displays the value and significance of the Spearman rank correlation between the seasonal NDJ values of the frequency and strength of CAP days and the corresponding averages (for maximum and minimum temperatures, wind speed, relative sunshine duration, and relative humidity) or accumulated values (for precipitation) of several climate variables recorded at Navacerrada and Barajas.

In general, the interannual variability in recent decades of parameters such as precipitation and relative sunshine duration, has been closely conditioned by the frequency of the atmospheric situations that generate

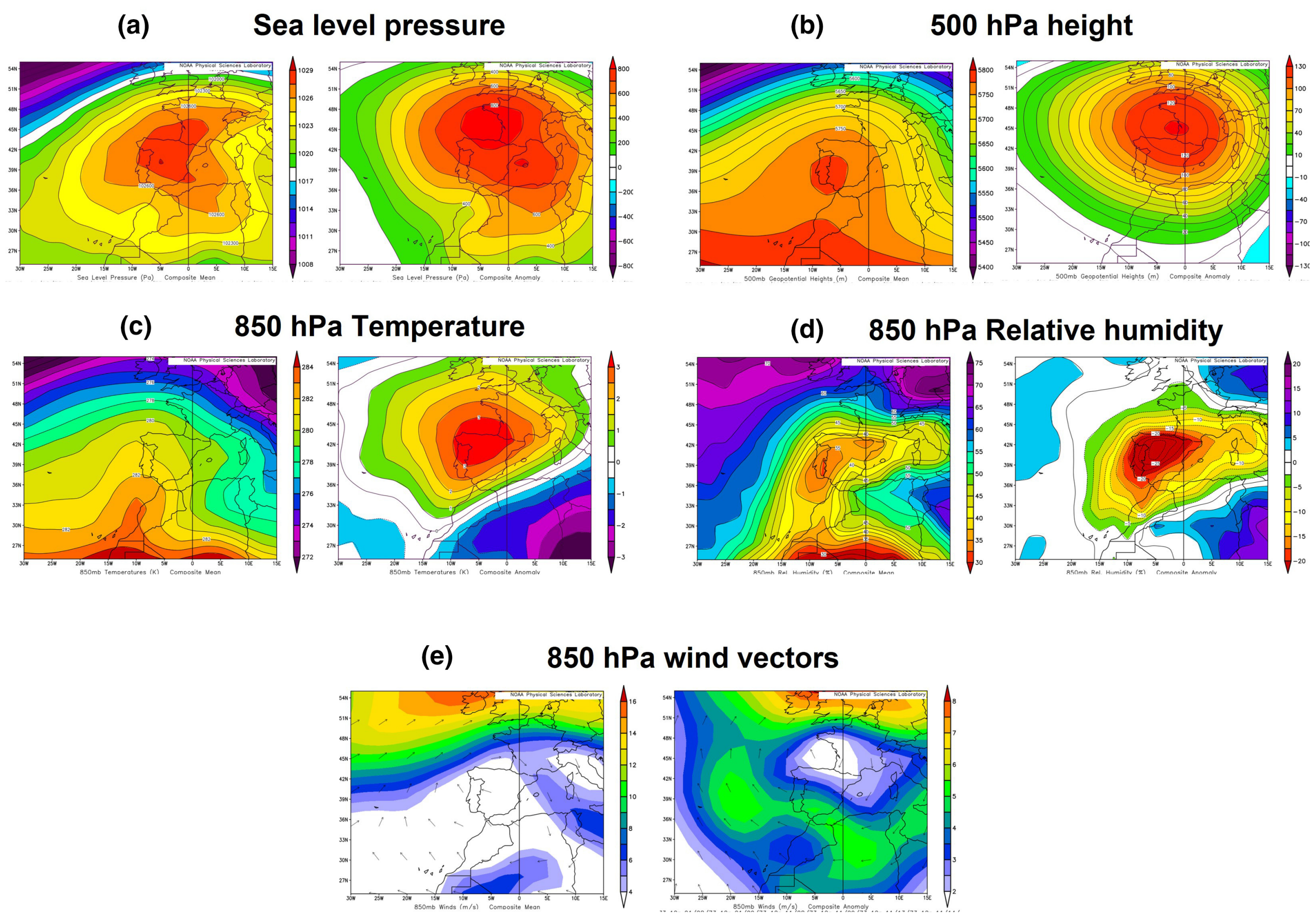

FIGURE 6 Composites and anomaly fields of (a) sea level pressure, (b) 500-hPa geopotential height (gpm), (c) air temperature at 850 hPa, (d) relative humidity at 850 hPa, and (e) wind vectors at 850 hPa corresponding to winter (NDJ, 1961–2020) CAP days. Image provided by the NOAA/ESRL Physical Sciences Laboratory from their web site at http://psl.noaa.gov [Colour figure can be viewed at wileyonlinelibrary.com]

TABLE 2 Spearman correlation coefficients between winter (NDJ, 1961-2020; 1961-2018 for Azores High parameters) CAP frequency, CAP strength and the same day difference in maximum temperature, and corresponding values of selected Northern Hemisphere teleconnection patterns

	NAO	EA	EA/WR	SCAND
CAP Frequency (days)	**0.65**	−0.19	0.23	**−0.41**
CAP strength (°C)	0.13	−0.20	0.06	−0.12
Same day difference in maximum temperature (°C)	0.02	0.12	0.07	0.06

Note: Seasonal values were averaged from monthly values. Significant correlations ($p \leq .05$) are highlighted in bold.

CAPs. Since most of the winter precipitation in our study area is usually provided by cyclonic disturbances, we may infer that the persistent anticyclones deviate the path of those storms northward, drastically reducing the frequency and amount of precipitation. Besides, regional-scale subsidence associated with those high-pressure cells generate clear skies and elevated values of sunshine duration and hence, solar radiation. The generalized conceptualization of CAP event implies clear-sky conditions; however, cold-air pools can sometimes lead to a different meteorological scenario, which explains the slightly lower correlation values between the frequency of CAPs and sunshine duration in Barajas. Episodes of radiative fog, which are most frequently at dawn, can persist the following morning when evolve towards low-level stratiform clouds. They are capable to inhibit the daytime warming at the plains, but also the subsequent night-time cooling, disrupting the typical dual pattern in boundary layer mixing (Whiteman *et al.*, 2001; Zhong *et al.*, 2001). Regarding relative humidity, a more complex relationship exists at Barajas (Figure 8a), where the usual contrasted daily cycle is enhanced during the daytime, meanwhile nocturnal values are closely like non-CAP days. On the contrary, two clearly contrasted humidity regimes appear during CAP days and non-CAP days at Navacerrada (Figure 8b): the average daily relative humidity during CAP days is approximately 42%; during non-CAP days is 88%.

Influence of CAP days on the long-term evolution of the regional temperatures is certainly complex. The frequency of CAP days maintains a positive but moderate relationship with maximum temperatures in both the plains and the mountains, consequence of the upper-level warm advection and the high levels of sunshine. By night, however, the influence weakens at Navacerrada and reverses at Barajas. Such behaviour can be explained looking at the hourly regime of temperatures in both sites. CAP days warm Barajas no more than 2.5°C by

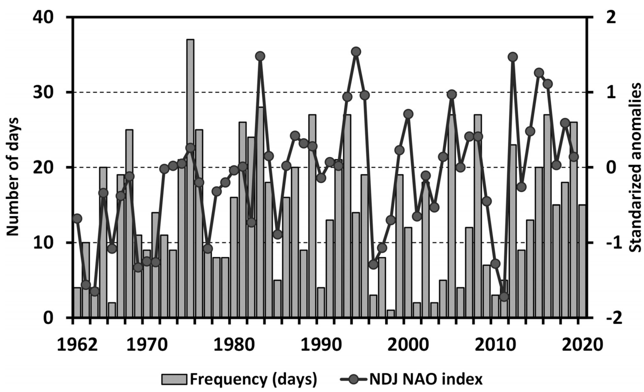

FIGURE 7 Interannual variability of winter (NDJ, 1961–2020) CAP days versus NAO index

daytime (with a delay of 2 hr regarding the maximum solar radiation), but the cooling is noticeably by night, well below the corresponding to no-CAP days (Figure 8c). Conversely, Navacerrada closely matches the daily course of solar radiation (the maximum temperature occurs at noon) but, once the sun disappears, the temperature displays a reduced variance (Figure 8d). Here, temperatures are dominated by the advection of a warm and subsident air mass, while its location in a small ridge precludes any additional cooling due to the accumulation of cold air.

CAP days have been pointed out as a driver of episodes of extreme night-time temperatures at the bottom of valleys worldwide (Wang *et al.*, 2015; Vitasse *et al.*, 2017), which is one of the thermal indices more sensible to global warming (IPCC, 2021). The value of the correlation between the frequency of CAP days and the number of days with extreme minimum temperatures is like the calculated for minimum temperatures (0.58, with a $p < .001$), thus suggesting that CAPs are not the only process involved in the genesis of very cold nights (Prieto *et al.*, 2002). For example, after storm "Philomena" the centre of the Iberian Peninsula experienced very cold nights (minimum temperatures of −25.2°C in Molina de Aragón on January 12). On the same morning, Barajas recorded a minimum of −12.6°C and Navacerrada −8.9°C. However, 5 days later, a strong temperature difference occurred when the mountain began to warm due to the arrival of a strong upper-level ridge (Navacerrada 0.8°C and Barajas −9.1°C). The evolution of the number of days with extreme minimum temperatures in Barajas shows a statistically significant downward trend (Table 4). However, when days are separated in two groups, the trend of those coinciding with CAPs is not significant.

TABLE 3 Spearman correlation coefficients (*rho*) between the winter (NDJ, 1961-2020) frequency and strength of CAP, same day difference in maximum temperature, and corresponding values of several climate parameters (*Tx* stands for maximum temperatures, *Tn* stands for minimum temperatures, *Ws* stands for wind speed, *Rh* stands for relative humidity, *Pp* stands for precipitation and *Sr* stands for sunshine ratio -% with respect to the maximum number of hours of potential sunshine-) at Navacerrada and Barajas

	Tx	Tn	Ws	Rh	Pp	Sr
Navacerrada (1894 m asl)						
CAP Frequency (days)	**0.59**	**0.38**	−0.26	**−0.86**	**−0.69**	**0.87**
Same day difference in maximum temperature (°C)	0.26	0.03	0.08	−0.23	−0.12	−0.02
CAP strength (°C)	0.23	0.15	−0.12	**−0.49**	**−0.35**	**0.35**
Barajas Airport (609 m asl)						
CAP Frequency (days)	**0.49**	**−0.64**	**−0.57**	**−0.48**	**−0.75**	**0.78**
Same day difference in maximum temperature (°C)	−0.19	0.00	0.02	0.13	−0.17	−0.02
CAP strength (°C)	0.11	−0.42	−0.31	−0.22	−0.45	0.32

Note: Significant correlations ($p \leq .05$) are highlighted in bold.

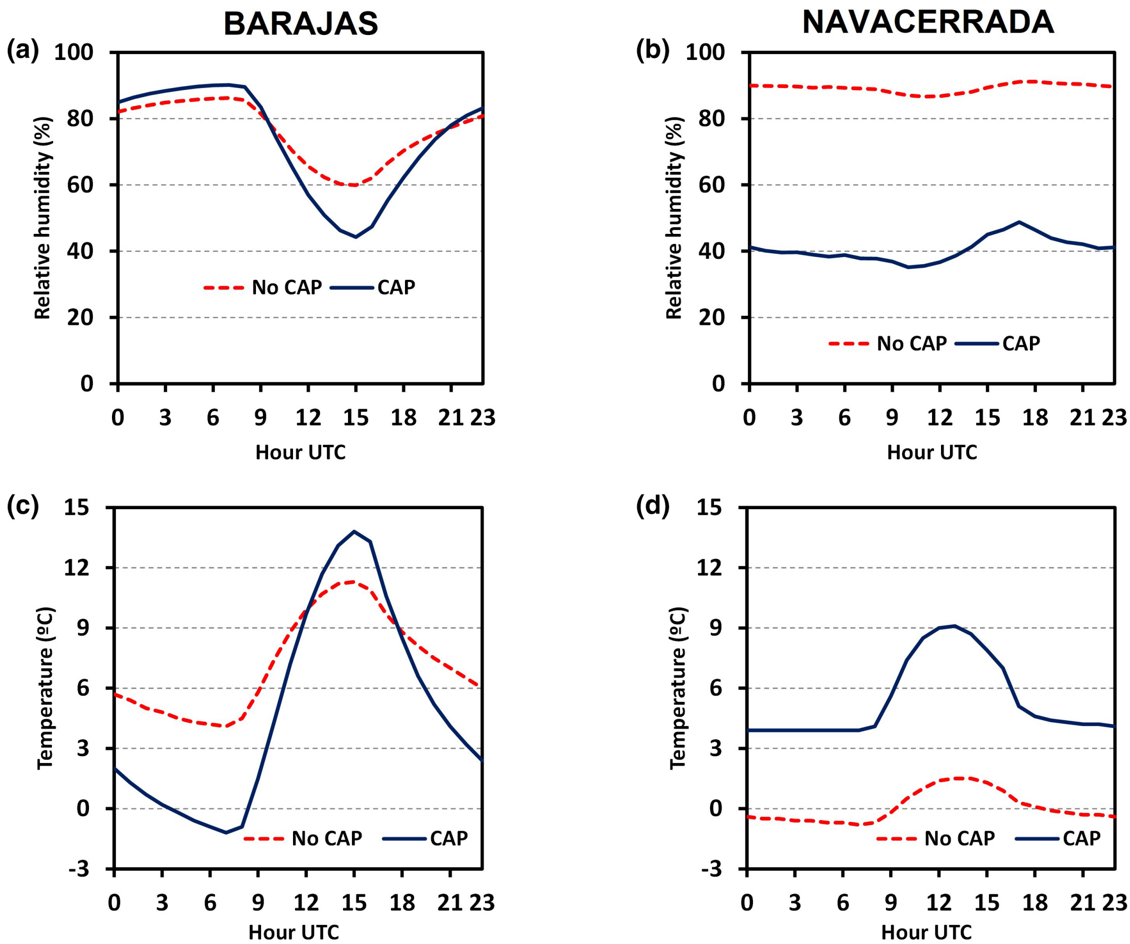

FIGURE 8 Hourly cycle of (a, b) relative humidity temperature and (c, d) temperature in Barajas (left) and Navacerrada (right) corresponding to winter (NDJ, 2012–2016) CAP and no CAP days [Colour figure can be viewed at wileyonlinelibrary.com]

With reference to wind speed (Figure 9a), the relationship is moderate in the case of Barajas, but not significant at the 95% confidence level at Navacerrada. While 90% of CAP days correspond to daily wind averages lower than 2 $m{\cdot}s^{-1}$ in Barajas, CAP days with winds between 4 and 10 $m{\cdot}s^{-1}$ have been still recorded at Navacerrada, most of the time due to the crossing of the southern tip of a cold front. Besides, an evident de-coupling between the surface and the summits is deduced from the wind roses (Figure 9b): at midnight, northerly (katabatic) winds predominate in Barajas versus southerlies in Navacerrada; at midday, the reversal is true: southerly (weaker anabatic flow) against northerly.

TABLE 4 *Z* statistic and significance from a Mann–Kendall trend test and *Q* (slope) and *β* (intercept) values of a Theil–Sen analysis on winter (NDJ, 1961–2020) values of the frequency of very cold nights (below the 95th percentile of daily winter minimum temperatures) in Barajas

	Z	Significance	*Q*	*β*
Frequency of very cold nights (all days)	−2.27	*	−0.143	18.43
Frequency of very cold nights during no CAP events	−2.51	*	−0.067	6.93
Frequency of very cold nights during CAP events	−1.17		−0.050	7.90

Note: * Trend at α = 0.05 level of significance.

4 | DISCUSSION AND CONCLUSIONS

The present study offers a climatology of cold air pools (CAP) over the southern Spanish Plateau and investigates its evolution since 1961 and their links with the regional climate trends. The lack of reliable and complete datasets of upper-air soundings or a dense network of meteorological stations in mountain areas is a serious handicap for the analysis of the long-term characteristics of CAP

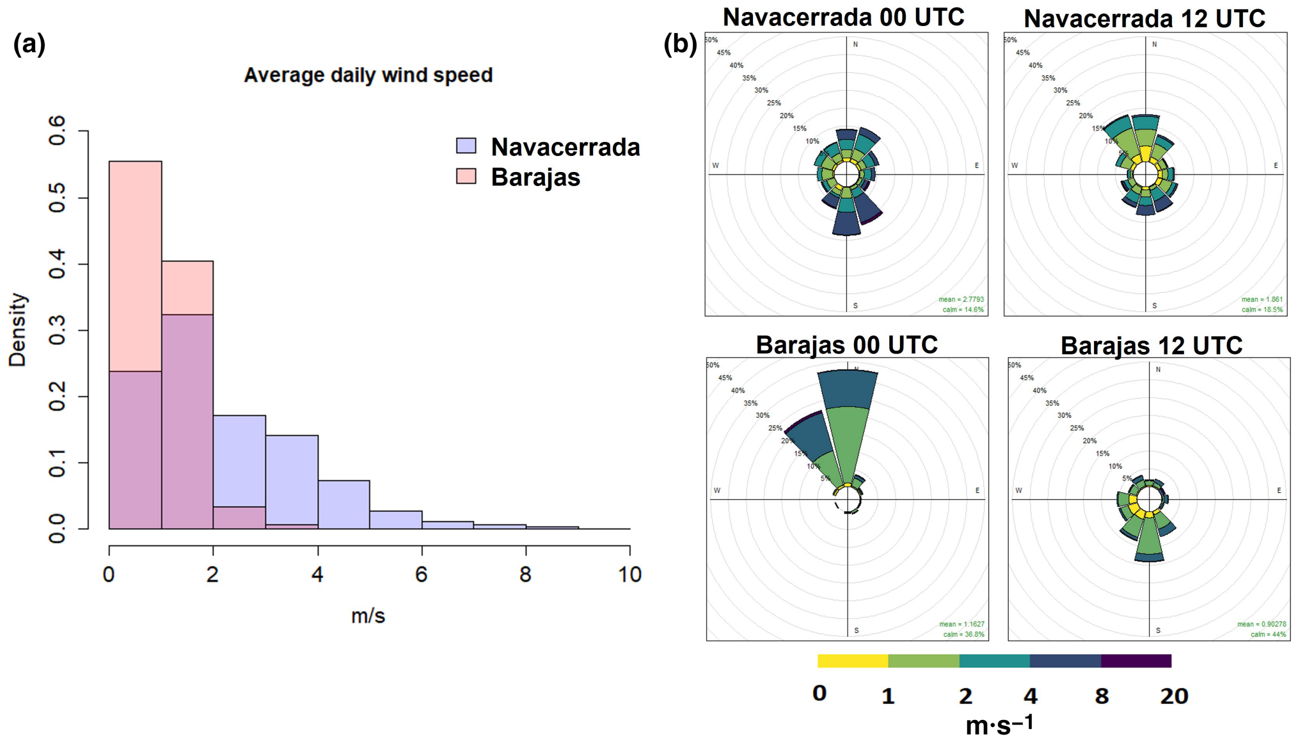

FIGURE 9 (a) Average daily values of wind speed and (b) wind roses at 0000 and 1200 UTC in Navacerrada and Barajas corresponding to winter (NDJ, 2012–2016) CAP days [Colour figure can be viewed at wileyonlinelibrary.com]

events. To cope with this problem, an alternative approach based on the comparison of long and consistent air temperature measurement from a pair of stations, one in the Sistema Central Range (Navacerrada, 1,894 m asl) and another in the plains (Madrid-Barajas, 609 m asl), has been applied to estimate the decadal variability in frequency and strength of CAPs in the southern Spanish Plateau. To test the representativeness of both stations to depict adequately the main features of CAPs in time and space, a well-proven method based on a EOF decomposition was applied over a shorter temporal period. A close agreement was found between the daily values of the synthetic index provided by the EOF procedure and the difference of minimum temperatures between Navacerrada and Barajas, better for winter months, when the daytime convective mixing is not too active (Whiteman *et al*., 2004).

CAPs were found to occur year-round about 39 days per year (10.74%), but they are most frequent in winter (NDJ), when sequences are longer and stronger. The top of that inversion layer forms up to an altitude of about 800–1,000 m, close to the average elevation of the piedmont. During this period of low radiative budget (low solar angles and longer nights), a topographic configuration, favourable to the stagnation of air masses set up the optimal conditions for those events. However, their lower frequency in comparison with other regions (Po Valley, Great Basin, Santiago Basin) can be explained not only by the definition of CAPs applied in this paper, but also by the easy access of the westerly circulation to the interior of the Iberian Peninsula. The narrowness of the topography in other regions prevents strong upper troposphere winds to penetrate in the bottom of the valleys, preserving longer CAPs (Miró *et al*., 2018). No temporal trends were found on the frequency of CAPs nor their strength, unlike daytime maximum temperatures which show a reduction explained by a differential warming trend in Navacerrada.

The seasonal cycle of CAPs is modulated by synoptic (upper air warm advection and subsidence), regional (katabatic flows), and local (radiative cooling) mechanisms. The most persistent and intense CAPs are developed when an anticyclone stagnates over the region, resulting from the expansion of the Azores High towards the Iberian Peninsula, linked to a well-defined positive NAO phase. When the NAO is in a positive phase both the subpolar Iceland Low and the subtropical Azores-Bermuda high are stronger than average. The increased difference in pressure between both two regions results in a stronger Atlantic jet stream and a northward shift of the storm track; southward, subsidence from the upper-level ridges dissipates cloudiness and minimizes the chance of precipitation. The spurious correlation between CAPs and the Scandinavia pattern (SCAND) probably result from the averaging process of the original monthly values. According to the Climate Prediction Center (https://www.cpc.ncep.noaa.gov/data/teledoc/telecontents.shtml), the Scandinavia pattern (SCAND) shows significant correlations with precipitation, but not with average temperature, in our study region. The SCAND pattern consists of a primary circulation centre over Scandinavia, with a weaker centre of opposite sign over Southern Europe. Its negative phase would be associated with negative height anomalies (deep lows) over Scandinavia and Western Russia but weak anticyclones southward.

Several studies have demonstrated the clear influence of large-scale atmospheric pressure patterns on the occurrence of CAPs. Gillies *et al.* (2010a, 2010b) linked persistent inversions in Utah's Salt Lake Valley to the two key modes, a synoptic (6-day) mode and an intra-seasonal (30-day) mode of the mid-latitude winter circulation over western United States. Wang *et al.* (2012, 2013, 2015) showed a coherent temporal pattern in temperature inversions at Caché Valley, in Utah, linked with decadal-scale climate trends associated with the NAO. Zhong *et al.* (2011) revealed a correlation between the interannual variation of weak persistent deep stable layers at the Great Basin and the MEI index, a composite El Niño–Southern Oscillation (ENSO) index. Finally, Vitasse *et al.* (2017) found CAP conditions highly correlated with the North Atlantic Oscillation and the East Atlantic indices at La Brevine Valley (Jura Mountains, Switzerland).

When comparing the seasonal frequency and strength of CAP days with time series of other climate variables recorded at Navacerrada and Barajas, interesting insights about its role on the recent regional climatic evolution arise. The effect is maximum over long-term precipitation and sunshine ratios (up to 60% of the variance shared) and spatially dependent for moisture: strong in the summits, where humidity is constantly low, but weaker at Barajas, where relative humidity remains rather high during night-time because saturation vapour pressure decreases when temperature drops. Fog occurrence may explain the lower correlation of sunshine ratios and minimum temperatures at Barajas (when a restricted radiative cooling prevents the nocturnal minima from reaching the low values typically observed during CAPs). The stability induced by anticyclones also limits wind speed, particularly in the plain; additionally, a decoupling from the regional circulation and the developing of a thermally driven circulation are observed: weak upslope (S to SE) anabatic winds by daytime and slightly stronger katabatic nocturnal winds (from NW to N). This behaviour is related to the differential strength of the daytime growth of the convective boundary layer and the warming (cooling) of the mountains under weak synoptic forcings (Román-Cascón *et al.*, 2019).

The atmospheric circulation prone to the genesis of CAPs have modulated the wintertime warming undergone by the interior of the Iberian Peninsula after 1961 on a complex way. Several studies have reported a warming since the beginning of the 20th century in Spain, accelerated from 1970s onwards (Brunet *et al.*, 2007). Barajas winter (DJF) maximum temperatures have warmed at essentially the same rate that the rest of the Iberian Peninsula, while the warming is differentially higher in the mountains. The most feasible cause of such differential warming between the plain and the mountain is a snow–ice feedback mechanism which can induce a rise of the 0°C isotherm due to the progressive reduction of the snow cover (Pepin and Lundquist, 2008). Predominance of anticyclonic circulations would induce a strong reduction of cloud cover; enhanced daytime solar short-wave radiation further increases the heating effect related with the warm air advection, while the strong nocturnal clear sky emission of long wave radiation partially offsets that advection by cooling the lower troposphere. Although there are not specific reports about the evolution of the snow cover at the mountains of the Sistema Central, studies from other Iberian Peninsula ranges (e.g., Morán-Tejeda *et al.*, 2013; Alonso-González *et al.*, 2019; López-Moreno *et al.*, 2020) display a coherent regional signal to conditions unfavourable to the persistence of the snowpack. Besides, over the last few years, evidence has accumulated of the influence of this recent climate evolution, particularly by warmer winters, less snowfall and shorter snow duration, on the landscape and fauna of the Sistema Central Range. For example, herbaceous plants, which are highly correlated with a long snow permanence and abundance of melting water, have been replaced by leguminous shrubs, which are steadily becoming denser (Sanz-Elorza *et al.*, 2003; Andrés *et al.*, 2007; García-Romero *et al.*, 2010), or butterflies, whose altitudinal range has rising on average 200 m during the last 35 years (Wilson *et al.*, 2007). Mountains are considered an unbiased natural laboratory of the global warming, although the signal on the recent evolution of vertical temperature gradients offers a mixture of magnitudes or even competing trends in mountains (the so-called elevation-dependent warming or EDW; Mountain Research Initiative EDW Working Group, 2015), suggesting that different mountain ranges can react in contrasting ways to that global trend, and within each range, summits and valleys may show divergent trends (Holden and Rose, 2011; Pepin *et al.*, 2011; Rangwala and Miller, 2012; Kirchner *et al.*, 2013; Wang *et al.*, 2014).

According to our results, the maintenance of CAP frequency and intensity could have contributed to a relative slowdown in any downward trend of the coldest days at Barajas which would have otherwise been expected to result from global warming. Changes in daily temperature extremes over Spain, using a range of percentile-based indices, confirm a general increase in the frequency of summer warm events and heat waves and a decrease in the frequency of winter cold events (García-Herrera *et al.*, 2005; Fernández-Montes and Rodrigo, 2012; El Kenawy *et al.*, 2013; Labajo *et al.*, 2014). However, a significant impact of CAPs in regional minimum temperature trends have been observed in some places, like the Great Basin of western United States. Here, the winter weather evolution has recorded a warming of the low troposphere since the middle of the 20th century, resulting into a larger rain to snowfall ratio at the mountains, while at the bottom of the valleys no warming trend was observed (Gillies *et al.*, 2012). Theoretically, in a warmer climate, a decrease in the frequency and intensity of cold nights is expected. For example, on the Iberian Peninsula, López-Moreno *et al.* (2014) advise of a continuous and significant increasing trend in occurrence of warm and very warm days and nights in the mountains (Pyrenees and Iberian Range) of the NE Iberian Peninsula, which in some cases, is projected to double during the period 2021–2050 and continue increasing for the period 2051–2080. But the global trends towards a warmer climate may not necessarily affect the intensity and duration of CAPs (Kodra *et al.*, 2011). Atmospheric circulation patterns that promote CAPs may become more prevalent as the atmosphere warms, since forced climate model projections with increasing greenhouse gas concentrations indicate a pattern of more anticyclonic conditions over latitudes like those of the Iberian Peninsula (Horton *et al.*, 2012; 2014). That scenario may favour the occurrence of cold air build-up and CAPs can even increase. In the Po Valley, Caserini *et al.* (2017) projected an increase of the occurrence of temperature inversions and stagnation events, less relevant under an extreme emissions scenario (RCP8.5) and concentrated in the warmer months. On the same line, Ji *et al.* (2019) found a substantial increase in the strength of near surface temperature inversions over southeast Australia due to the dominant role of the large-scale circulation. Besides, changes in the daytime variability indicate that near surface layers will be less stable in the afternoon leading to conditions favouring convective systems and more stable in the early morning which is favourable for temperature inversions. Such evolution, in case of persist, might mitigate some of the adverse effects of global warming by maintaining suitable microclimatic conditions for endangered species and ecosystems, particularly in mountainous regions (Dobrowski *et al.*, 2009; Dobrowski, 2011; Curtis *et al.*, 2014; Morelli *et al.*, 2016; Rupp *et al.*, 2020) but would become a bad scenario for air quality issues. Climate model simulations have suggested that southern Europe is likely to experience a higher incidence of positive North Atlantic Oscillation states in the future and a large eastward shift of both North Atlantic sea-level pressure centres of action, combined with more frequent mid-latitude blocking and a northward shift of the jet stream. All these atmospheric circulation changes would increase the frequency of stagnant air masses over urban centres and the consequent degradation of air quality, increasing the $PM_{2.5}$ concentrations beyond the World Health Organization Air Quality Guidelines (Messori *et al.*, 2018).

Such impacts invite to further assess the role of CAPs under future climate scenarios of enhanced large-scale stable (anticyclonic) conditions, its implications for air quality in urban agglomerations, and promotes the need to consider singular responses at local scales in the framework of the global climate warming.

ACKNOWLEDGMENTS

We thank AeMet (Spanish Meteorology Agency) for providing the data that has allowed this work to be carried out. The comments of two reviewers are deeply appreciated, having served to substantially improve this paper.

FUNDING INFORMATION

Research project "*Analisis y modelizacion de eventos climaticos extremos en Madrid: olas de calor e inversiones termicas*" (Ref. CGL2016-80154-R). CICYT program, Ministerio de Economía y Competitividad. Gobierno de España.

ORCID

Domingo F. Rasilla https://orcid.org/0000-0003-2965-2822

REFERENCES

Alexandersson, H. (1986) A homogeneity test applied to precipitation data. *Journal of Climatology*, 6, 661–675. https://doi.org/10.1002/joc.3370060607.

Alonso-González, E., López-Moreno, J.I., Navarro-Serrano, F. and Revuelto, J. (2019) Impact of North Atlantic Oscillation on the snowpack in Iberian Peninsula Mountains. *Water*, 12, 105. https://doi.org/10.3390/w12010105.

Andrés, N., García-Romero, A. and Jiménez, J. (2007) Control of snow cover duration in geomorphologic and biogeographic dynamics in Mediterranean mountains: Manzanares valley head, Sierra de Guadarrama (Spain). *Zeitschrift für Geomorphologie*, 51, 91–111. https://doi.org/10.1127/0372-8854/2007/0051S2-0091.

Bailey, A., Chase, T., Cassano, J. and Noone, D. (2011) Changing temperature inversion characteristics in the U.S. southwest and relationships to large-scale atmospheric circulation. *Journal of Applied Meteorology and Climatology*, 50, 1307–1323. https://doi.org/10.1175/2011JAMC2584.1.

Bărcăcianu, F. and Apostol, L. (2014) Considerations on temperature inversions in the lower troposphere in the 2001–2002 cold season, south of the Carpathian Mountains. *Present Environment and Sustainable Development*, 8, 243–253. https://doi.org/10.2478/pesd-2014-0038.

Barry, R. (2008) *Mountain Weather and Climate*. Cambridge: Cambridge University Press, 506 pp. https://doi.org/10.1017/CBO9780511754753.

Beard, J., Beck, C., Graham, R., Packham, S., Traphagan, M., Giles, R. and Morgan, J. (2012) Winter temperature inversions and emergency department visits for asthma in Salt Lake County, Utah, 2003–2008. *Environmental Health Perspectives*, 120, 1385–1390. https://doi.org/10.1289/ehp.1104349.

Blennow, K. and Lindkvist, L. (2000) Models of low temperature and high irradiance and their application to explaining the risk of seedling mortality. *Forest Ecology and Management*, 135, 289–301. https://doi.org/10.1016/S0378-1127(00)00287-5.

Borge, R., Artíñano, B., Yagüe, C., Gomez-Moreno, F.J., Saiz-Lopez, A., Sastre, M., Narros, A., García-Nieto, D., Benavent, N., Maqueda, G., Barreiro, M., de Andrés, J.M. and Cristóbal, A. (2018) Application of a short-term air quality action plan in Madrid (Spain) under a high-pollution episode—part I: diagnostic and analysis from observations. *Science of the Total Environment*, 635, 1561–1573. https://doi.org/10.1016/j.scitotenv.2018.03.149.

Brunet, M., Jones, P.D., Sigró, J., Saladié, O., Aguilar, E., Moberg, A., Della-Marta, P.M., Lister, D., Walther, A. and López, D. (2007) Temporal and spatial temperature variability and change over Spain during 1850–2005. *Journal of Geophysical Research*, 112, D12117. https://doi.org/10.1029/2006JD008249.

Burns, P. and Chemel, C. (2014) Evolution of cold-air-pooling processes in complex terrain. *Boundary-Layer Meteorology*, 150, 423–447. https://doi.org/10.1007/s10546-013-9885-z.

Caserini, S., Giani, P., Cacciamani, C., Ozgen, S. and Lonati, G. (2017) Influence of climate change on the frequency of daytime temperature inversions and stagnation events in the Po Valley: historical trend and future projections. *Atmospheric Research*, 184, 15–23. https://doi.org/10.1016/j.atmosres.2016.09.018.

Chachere, C. and Pu, Z. (2019) Numerical simulations of an inversion fog event in the Salt Lake Valley during the MATERHORN-fog field campaign. *Pure and Applied Geophysics*, 176, 2139–2164. https://doi.org/10.1007/s00024-018-1770-8.

Chemel, C., Arduini, G., Staquet, C., Largeron, Y., Legain, D., Tzanos, D. and Paci, A. (2016) Valley heat deficit as a bulk measure of wintertime particulate air pollution in the Arve River Valley. *Atmospheric Environment*, 128, 208–215. https://doi.org/10.1016/j.atmosenv.2015.12.058.

Chemel, C. and Burns, P. (2015) Pollutant dispersion in a developing valley cold-air pool. *Boundary-Layer Meteorology*, 154, 391–408. https://doi.org/10.1007/s10546-014-9984-5.

Clements, C.B., Whiteman, C.D. and Horel, J.D. (2003) Cold-air-pool structure and evolution in a mountain basin: Peter Sinks, Utah. *Journal of Applied Meteorology*, 42, 752–768.

Curtis, J., Flint, L.E., Flint, A.L., Lundquist, J.D., Hudgens, B., Boydston, E.E. and Young, J.K. (2014) Incorporating cold-air pooling into downscaled climate models increases potential refugia for snow-dependent species within the Sierra Nevada ecoregion, CA. *PLoS ONE*, 9, e106984. https://doi.org/10.1371/journal.pone.0106984.

Dai, A., Wang, J., Thorne, P., Parker, D., Haimberger, L. and Wang, X. (2011) A new approach to homogenize daily radiosonde humidity data. *Journal of Climate*, 24, 965–991. https://doi.org/10.1175/2010JCLI3816.1.

Daly, C., Conklin, D. and Unsworth, M. (2009) Local atmospheric coupling in complex topography alters climate change impacts. *International Journal of Climatology*, 30, 1857–1864. https://doi.org/10.1002/joc.2007.

Dobrowski, S.Z. (2011) A climatic basis for microrefugia: the influence of terrain on climate. *Global Change Biology*, 17, 1022–1035. https://doi.org/10.1111/j.1365-2486.2010.02263.x.

Dobrowski, S.Z., Abatzoglou, J.T., Greenberg, J.A. and Schladow, S.G. (2009) How much influence does landscape-scale physiography have on air temperature in a mountain environment? *Agricultural and Forest Meteorology*, 149, 1751–1758. https://doi.org/10.1016/j.agrformet.2009.06.006.

Durre, I., Yin, X., Vose, R., Applequist, S. and Arnfield, J. (2018) Enhancing the data coverage in the integrated global radiosonde archive. *Journal of Atmospheric and Oceanic Technology*, 35, 1753–1770. https://doi.org/10.1175/JTECH-D-17-0223.1.

El Kenawy, A., López-Moreno, J.I., Brunsell, N.A. and Vicente-Serrano, S.M. (2013) Anomalously severe cold nights and warm days in northeastern Spain: their spatial variability, driving forces and future projections. *Global and Planetary Change*, 101, 12–32. https://doi.org/10.1016/j.gloplacha.2012.11.011.

Espín Sánchez, D. (2015) Riesgo de heladas por inversión térmica en la Huerta de Murcia: incidencia en la actividad agraria. *Investigaciones Geográficas*, 64, 73–86. https://doi.org/10.14198/INGEO2015.64.05.

Fernández-Montes, S. and Rodrigo, F.S. (2012) Trends in seasonal indices of daily temperature extremes in the Iberian Peninsula, 1929–2005. *International Journal of Climatology*, 32, 2320–2332. https://doi.org/10.1002/joc.3399.

Flores, F., Arriagada, A., Donoso, N., Martínez, A., Viscarra, A., Falvey, M. and Schmitz, R. (2020) Investigation of a nocturnal cold-air pool in a semiclosed basin located in the Atacama Desert. *Journal of Applied Meteorology and Climatology*, 59, 1–48. https://doi.org/10.1175/JAMC-D-19-0237.1.

García-Herrera, R., Díaz, J., Trigo, R.M. and Hernández, E. (2005) Extreme summer temperatures in Iberia: health impacts and associated synoptic conditions. *Annals Geophysicae*, 23, 239–251. https://doi.org/10.5194/angeo-23-239-2005.

García-Romero, A., Muñoz, J., Andrés, N. and Palacios, D. (2010) Relationship between climate change and vegetation distribution in the Mediterranean mountains: Manzanares Head valley, Sierra de Guadarrama (Central Spain). *Climatic Change*, 100, 645–666. https://doi.org/10.1007/s10584-009-9727-7.

Gillies, R.R., Wang, S.-Y. and Booth, M.R. (2010a) Atmospheric scale interaction on wintertime Intermountain west low-level inversions. *Weather and Forecasting*, 25, 1196–1210. https://doi.org/10.1175/2010WAF2222380.1.

Gillies, R.R., Wang, S.-Y., Yoon, J.-H. and Weaver, S. (2010b) CFS prediction of winter persistent inversions in the Intermountain region. *Weather and Forecasting*, 25, 1211–1218. https://doi.org/10.1175/2010WAF2222419.1.

Gramsch, E., Cáceres, D., Oyola, P., Reyes, F., Vásquez, Y., Rubio, M.A. and Sánchez, G. (2014) Influence of surface and subsidence thermal inversion on PM2.5 and black carbon concentration. *Atmospheric Environment*, 98, 290–298. https://doi.org/10.1016/j.atmosenv.2014.08.066.

Gillies, R., Wang, S.Y. and Booth, M. (2012) Observational and synoptic analyses of the winter precipitation regime change over Utah. *J. Climate,* 25, 4679-4698. https://10.1175/JCLI-D-11-00084.1

Green, M.C., Chow, J.C., Watson, J.G., Dick, K. and Inouye, D. (2015) Effect of snow cover and atmospheric stability on winter PM2.5 concentrations in western U.S. valleys. *Journal of Applied Meteorology and Climatology*, 54, 1191–1201. https://doi.org/10.1175/JAMC-D-14-0191.1.

Haimberger, L. (2007) Homogenization of radiosonde temperature time series using innovation statistics. *Journal of Climate*, 20, 1377–1403. https://doi.org/10.1175/JCLI4050.1.

Hiebl, J. and Schöner, W. (2018) Temperature inversions in Austria in a warming climate change in space and time. *Meteorologische Zeitschrift*, 27, 309–323. https://doi.org/10.1127/metz/2018/0899.

Hodges, D. and Pu, Z. (2016) The climatology, frequency, and distribution of cold season fog events in northern Utah. *Pure and Applied Geophysics*, 173, 3197–3211. https://doi.org/10.1007/s00024-015-1187-6.

Holden, J. and Rose, R. (2011) Temperature and surface lapse rate change: a study of the UK's longest upland instrumental record. *International Journal of Climatology*, 31, 907–919. https://doi.org/10.1002/joc.2136.

Holman, C., Harrison, R. and Querol, X. (2015) Review of the efficacy of low emission zones to improve urban air quality in European cities. *Atmospheric Environment*, 111, 161–169. https://doi.org/10.1016/j.atmosenv.2015.04.009.

Horton, D., Harshvardhan, E. and Diffenbaugh, N.S. (2012) Response of air stagnation frequency to anthropogenically enhanced radiative forcing. *Environmental Research Letters*, 7, 044034. https://doi.org/10.1088/1748-9326/7/4/044034.

Horton, D., Skinner, C., Singh, D. and Diffenbaugh, N. (2014) Occurrence and persistence of future atmospheric stagnation events. *Nature Climate Change*, 4, 698–703. https://doi.org/10.1038/nclimate2272.

IPCC. (2021) Summary for policymakers. In: Masson-Delmotte, V. P., Zhai, A., Pirani, S.L., Connors, C., Péan, S., Berger, N., Caud, Y., Chen, L., Goldfarb, M.I. and Gomis, M. (Eds.) *Climate Change 2021: The Physical Science Basis. Contribution of Working Group I to the Sixth Assessment Report of the Intergovernmental Panel on Climate Change*. Cambridge: Cambridge University Press.

Ivey, C.E., Balachandran, S., Colgan, S., Hu, Y. and Holmes, H.A. (2019) Investigating fine particulate matter sources in Salt Lake City during persistent cold air pool events. *Atmospheric Environment*, 213, 568–578. https://doi.org/10.1016/j.atmosenv.2019.06.042.

Ji, F., Evans, J., Di Luca, A., Jiang, N., Olson, R., Fita, L., Argueso, D., Chang, L., Scorgie, Y. and Riley, M. (2019) Projected change in characteristics of near surface temperature inversions for Southeast Australia. *Climate Dynamics*, 52, 1487–1503. https://doi.org/10.1007/s00382-018-4214-3.

Joly, D. and Richard, J.Y. (2019) Frequency, intensity, and duration of thermal inversions in the Jura Mountains of France. *Theoretical and Applied Climatology*, 138, 639–655. https://doi.org/10.1007/s00704-019-02855-3.

Kalnay, E., Kanamitsu, M., Kistler, R., Collins, W., Deaven, D., Gandin, L.S., Iredell, M., Saha, S., White, G., Woollen, J., Zhu, Y., Chelliah, M., Ebisuzaki, W., Higgins, W., Janowiak, J., Ropelewski, C., Wang, J. and Leetmaa, A. (1996) The NMC/NCAR 40-year reanalysis project. *Bulletin of the American Meteorological Society*, 77, 437–471. https://doi.org/10.1175/1520-0477(1996)077<0437:TNYRP>2.0.CO;2.

Kendall, M.G. (1975) *Rank Correlation Methods*. London: Charles Griffin.

Kikaj, D., Vaupotič, J. and Chambers, S. (2019) Identifying persistent temperature inversion events in a subalpine basin using radon-222. *Atmospheric Measurement Techniques*, 12, 4455–4477. https://doi.org/10.5194/amt-12-4455-2019.

Kirchner, M., Faus-Kessler, T., Jakobi, G., Leuchner, M., Ries, L., Scheel, H.E. and Suppan, P. (2013) Altitudinal temperature lapse rates in an Alpine valley: trends and the influence of season and weather patterns. *International Journal of Climatology*, 33, 539–555. https://doi.org/10.1002/joc.3444.

Kodra, E., Steinhaeuser, K. and Ganguly, A. (2011) Persisting cold extremes under 21st century warming scenarios. *Geophysical Research Letters*, 38, L08705. https://doi.org/10.1029/2011GL047103.

Kottek, M., Grieser, J., Beck, C., Rudolf, B. and Rubel, F. (2006) World map of the Köppen–Geiger climate classification updated. *Meteorologische Zeitschrift*, 15, 259–263. https://doi.org/10.1127/0941-2948/2006/0130.

Labajo, A.L., Egido, M., Martín, Q., Labajo, J. and Labajo, J.L. (2014) Definition and temporal evolution of the heat and cold waves over the Spanish Central Plateau from 1961 to 2010. *Atmosfera*, 27, 273–286.

Lareau, N.P., Crosman, E., Whiteman, C.D., Horel, J.D., Hoch, S. W., Brown, W.O.J. and Horst, T.W. (2013) The persistent cold-air pool study. *Bulletin of the American Meteorological Society*, 94, 51–63. https://doi.org/10.1175/BAMS-D-11-00255.1.

Largeron, Y. and Staquet, C. (2016a) Persistent inversion dynamics and wintertime PM10 air pollution in Alpine valleys. *Atmospheric Environment*, 135, 92–108. https://doi.org/10.1016/j.atmosenv.2016.03.045.

Largeron, Y. and Staquet, C. (2016b) The atmospheric boundary layer during wintertime persistent inversions in the Grenoble valleys. *Frontiers in Earth Sciences*, 4, 70. https://doi.org/10.3389/feart.2016.00070.

Lehner, M., Whiteman, C.D. and Dorninger, M. (2017) Inversion build-up and cold-air outflow in a small Alpine sinkhole. *Boundary Layer Meteorology*, 163, 497–522. https://doi.org/10.1007/s10546-017-0232-7.

Lehner, M., Whiteman, C.D., Hoch, S.W., Jensen, D., Pardyjak, E. R., Leo, L.S., Di Sabatino, S. and Fernando, J.S. (2015) A case study of the nocturnal boundary layer evolution on a slope at the foot of a desert mountain. *Journal of Applied Meteorology and Climatology*, 54, 732–751. https://doi.org/10.1175/JAMC-D-14-0223.1.

Leukauf, D., Gohm, A., Rotach, M.W. and Wagner, J.S. (2015) The impact of the temperature inversion breakup on the exchange of heat and mass in an idealized valley: sensitivity to the radiative forcing. *Journal of Applied Meteorology and Climatology*, 54, 2199–2216. https://doi.org/10.1175/JAMC-D-15-0091.1.

López-Moreno, J.I., El-Kenawy, A., Revuelto, J., Azorín-Molina, C., Morán-Tejeda, E., Lorenzo-Lacruz, J., Zabalza, J. and Vicente-Serrano, S.M. (2014) Observed trends and future projections for winter warm events in the Ebro basin, Northeast Iberian Peninsula. *International Journal of Climatology*, 34, 49–60. https://doi.org/10.1002/joc.3665.

López-Moreno, J.I., Soubeyroux, J.M., Gascoin, S., Alonso-Gonzalez, E., Durán-Gómez, N., Lafaysse, M., Vernay, M., Carmagnola, C. and Morin, S. (2020) Long-term trends (1958–2017) in snow cover duration and depth in the Pyrenees. *International Journal of Climatology*, 40, 6122–6136. https://doi.org/10.1002/joc.6571.

Lu, W. and Zhong, S. (2014) A numerical study of a persistent cold air pool episode in the Salt Lake Valley, Utah. *Journal of Geophysical Research: Atmospheres*, 119, 1733–1752. https://doi.org/10.1002/2013JD020410.

Lundquist, J.D. and Cayan, D.R. (2007) Surface temperature patterns in complex terrain: daily variations and long-term change in the central Sierra Nevada, California. *Journal of Geophysical Research: Atmospheres*, 112, D11124. https://doi.org/10.1029/2006JD007561.

Lundquist, J.D., Pepin, N.C. and Rochford, C. (2008) Automated algorithm for mapping regions of cold-air pooling in complex terrain. *Journal of Geophysical Research: Atmospheres*, 113, D22107. https://doi.org/10.1029/2008JD009879.

McCaffrey, K., Wilczak, J., Bianco, L., Grimit, E., Sharp, J., Banta, R., Friedrich, K., Fernando, H.J.S., Krishnamurthy, R., Leo, L. and Muradyan, P. (2019) Identification and characterization of persistent cold pool events from temperature and wind profilers in the Columbia River basin. *Journal of Applied Meteorology and Climatology*, 58, 2533–2551. https://doi.org/10.1175/JAMC-D-19-0046.1.

Messori, G., van Wees, D., Pausata, F., Acosta, J.C., Hannachi, A. and Dentener, F.J. (2018) The impact of future atmospheric circulation changes over the Euro-Atlantic sector on urban PM2.5 concentrations. *Tellus B: Chemical and Physical Meteorology*, 70, 1–22. https://doi.org/10.1080/16000889.2018.1468704.

Miró, J., Peña, J., Pepin, N., Sairouni, A. and Montserrat, A. (2018) Key features of cold-air pool episodes in the northeast of the Iberian Peninsula (Cerdanya, eastern Pyrenees). *International Journal of Climatology*, 38, 1105–1115. https://doi.org/10.1002/joc.5236.

Morán-Tejeda, E., Herrera, S., López-Moreno, I., Revuelto, J., Lehmann, A. and Beniston, M. (2013) Evolution and frequency (1970–2007) of combined temperature–precipitation modes in the Spanish mountains and sensitivity of snow cover. *Regional Environmental Change*, 13, 873–885. https://doi.org/10.1007/s10113-012-0380-8.

Morelli, T.L., Daly, C., Dobrowski, S.Z., Dulen, D.M., Ebersole, J.L., Jackson, S.T., Lundquist, J.D., Millar, C.I., Maher, S.P., Monahan, W.B., Nydick, K.R., Redmond, K.T., Sawyer, S.C., Stock, S. and Beissinger, S.R. (2016) Managing climate change refugia for climate adaptation. *PLoS One*, 11, e0159909. https://doi.org/10.1371/journal.pone.0159909.

Mountain Research Initiative EDW Working Group. (2015) Elevation-dependent warming in mountain regions of the world. *Nature Climate Change*, 5, 424–430. https://doi.org/10.1038/nclimate2563.

Navarro-Serrano, F., López-Moreno, J., Azorin-Molina, C., Alonso-González, E., Tomás-Burguera, M., Sanmiguel-Vallelado, A., Revuelto, J. and Vicente-Serrano, S.M. (2018) Estimation of near-surface air temperature lapse rates over continental Spain and its mountain areas. *International Journal of Climatology*, 38, 3233–3249. https://doi.org/10.1002/joc.5497.

Pagès, M., Pepin, N. and Miró, J. (2017) Measurement and modelling of temperature cold pools in the Cerdanya valley (Pyrenees), Spain. *Meteorological Applications*, 24, 290–302. https://doi.org/10.1002/met.1630.

Palarz, A., Celiński-Mysław, D. and Ustrnul, Z. (2019) Temporal and spatial variability of elevated inversions over Europe based on ERA-Interim reanalysis. *International Journal of Climatology*, 40, 1335–1347. https://doi.org/10.1002/joc.6271.

Palarz, A., Luterbacher, J., Ustrnul, Z., Xoplaki, E. and Celiński-Mysław, D. (2020) Representation of low-tropospheric temperature inversions in ECMWF reanalyses over Europe. *Environmental Research Letters*, 15, 074043. https://doi.org/10.1088/1748-9326/ab7d5d.

Palmieri, S., Durante, G., Siani, A.M. and Casale, G.R. (2008) Atmospheric stagnation episodes and hospital admissions. *Public Health*, 122, 1128–1130. https://doi.org/10.1016/j.puhe.2008.02.006.

Pepin, N.C. (2001) Lapse rate changes in northern England. *Theoretical and Applied Climatology*, 68, 1–16. https://doi.org/10.1007/s007040170049.

Pepin, N.C., Daly, C. and Lundquist, J. (2011) The influence of surface versus free-air decoupling on temperature trend patterns in the western United States. *Journal of Geophysical Research*, 116, D10109. https://doi.org/10.1029/2010JD014769.

Pepin, N.C. and Lundquist, J.D. (2008) Temperature trends at high elevations: patterns across the globe. *Geophysical Research Letters*, 35, L14701. https://doi.org/10.1029/2008GL034026.

Price, J., Vosper, S., Brown, A., Ross, A., Clark, P., Davies, F., Horlacher, V., Claxton, B., McGregor, J., Hoare, J., Jemmett-Smith, B. and Sheridan, P. (2011) COLPEX: field and numerical studies over a region of small hills. *Bulletin of the American Meteorological Society*, 92, 1636–1650. https://doi.org/10.1175/2011BAMS3032.1.

Prieto, L., García-Herrera, R., Díaz, J., Hernández, E. and Teso, T. (2002) NAO influence on extreme winter temperatures in Madrid (Spain). *Annales Geophysicae*, 20, 2077–2085. https://doi.org/10.5194/angeo-20-2077-2002.

Rangwala, I. and Miller, J. (2012) Climate change in mountains: a review of elevation-dependent warming and its possible causes. *Climatic Change*, 114, 527–547. https://doi.org/10.1007/s10584-012-0419-3.

Rolland, C. (2003) Spatial and seasonal variations of air temperature lapse rates in alpine regions. *Journal of Climate*, 16, 1032–1046. https://doi.org/10.1175/1520-0442(2003)016<1032:SASVOA>2.0.CO;2.

Román-Cascón, C., Yagüe, C., Arrillaga, J.A., Lothon, M., Pardyjak, E.R., Lohou, F., Inclán, R.M., Sastre, M., Maqueda, G., Derrien, S., Meyerfeld, Y., Hang, C., Campargue-Rodríguez, P. and Turki, I. (2019) Comparing mountain breezes and their impacts on CO_2 mixing ratios at three contrasting areas. *Atmospheric Research*, 221, 111–126. https://doi.org/10.1016/j.atmosres.2019.01.019.

Romero, F., Gomez, J., Rangel, T. and Vassallo, J.N. (2019) Impact of restrictions to tackle high pollution episodes in Madrid: modal share change in commuting corridors. *Transportation Research Part D: Transport and Environment*, 77, 77–91. https://doi.org/10.1016/j.trd.2019.10.021.

Rupp, D., Shafer, S., Daly, C., Jones, J. and Frey, S. (2020) Temperature gradients and inversions in a forested cascade range basin: synoptic- to local-scale controls. *Journal of Geophysical Research: Atmospheres*, 125, e2020JD032686. https://doi.org/10.1029/2020JD032686.

Salas, R., Villadóniga, M., Prieto-Rodriguez, J. and Russo, A. (2021) Were traffic restrictions in Madrid effective at reducing NO_2 levels? *Transportation Research Part D: Transport and Environment*, 91, 102689. https://doi.org/10.1016/j.trd.2020.102689.

Sanz-Elorza, M., Dana, E.D., González, A. and Sobrino, E. (2003) Changes in the high-mountain vegetation of the Central Iberian Peninsula as a probable sign of climate warming. *Annals of Botany*, 92, 273–280. https://doi.org/10.1093/aob/mcg130.

Schmidli, J., Poulos, G.S., Daniels, M.H. and Chow, F.K. (2009) External influences on nocturnal thermally driven flows in a deep valley. *Journal of Applied Meteorology and Climatology*, 48, 3–23. https://doi.org/10.1175/2008JAMC1852.1.

Schnitzhofer, R., Norman, M., Wisthaler, A., Vergeiner, J., Harnisch, F., Gohm, A., Obleitner, F., Fix, A., Neininger, B. and Hansel, A. (2009) A multimethodological approach to study the spatial distribution of air pollution in an Alpine valley during wintertime. *Atmospheric Chemistry and Physics*, 9, 3385–3396. https://doi.org/10.5194/acp-9-3385-2009.

Sen, P.K. (1968) Estimates of the regression coefficient based on Kendall's tau. *Journal of the American Statistical Association*, 63, 1379–1389. https://doi.org/10.2307/2285891.

Sheridan, P., Vosper, S. and Brown, A. (2014) Characteristics of cold pools observed in narrow valleys and dependence on external conditions. *Quarterly Journal of the Royal Meteorological Society*, 140, 715–728. https://doi.org/10.1002/qj.2159.

Silcox, G.D., Kelly, K.E., Crosman, E.T., Whiteman, C.D. and Allen, B.L. (2012) Wintertime PM2.5 concentrations during persistent, multi-day cold-air pools in a mountain valley. *Atmospheric Environment*, 46, 17–24. https://doi.org/10.1016/j.atmosenv.2011.10.041.

Steinacker, R., Whiteman, C.D., Dorninger, M., Pospichal, B., Eisenbach, S., Holzer, A.M., Weihs, P., Mursch-Radlgruber, E. and Baumann, K. (2007) A sinkhole field experiment in the eastern Alps. *Bulletin American Meteorological Society*, 88, 701–716. https://doi.org/10.1175/BAMS-88-5-701.

Tingting, X., Bing, L., Minsi, Z., Yu, S., Ling, K., Tiantian, W., Mingxu, L., Xuhui, C., Hongsheng, Z. and Tong, Z. (2021) Temperature inversions in China derived from sounding data from 1976 to 2015. *Tellus B: Chemical and Physical Meteorology*, 73, 1–18. https://doi.org/10.1080/16000889.2021.1898906.

Vitasse, Y., Klein, G., Kirchner, J. and Rebetez, M. (2017) Intensity, frequency and spatial configuration of winter temperature inversions in the closed La Brevine valley, Switzerland. *Theoretical and Applied Climatology*, 130, 1073–1083. https://doi.org/10.1007/s00704-016-1944-1.

Wang, Q., Fan, X. and Wang, M. (2014) Recent warming amplification over high elevation regions across the globe. *Climate Dynamics*, 43, 87–101. https://doi.org/10.1007/s00382-013-1889-3.

Wang, S.-Y., Gillies, R.R., Martin, R., Davies, R.E. and Booth, M. R. (2012) Connecting sub-seasonal movements of the winter mean ridge in western North America to inversion climatology in Cache Valley, Utah. *Journal of Applied Climatology*, 51, 617–627. https://doi.org/10.1175/JAMC-D-11-0101.1.

Wang, S.-Y., Gillies, R.R. and van den Dool, H. (2013) On the yearly phase delay of winter intra-seasonal mode in the western United States. *Climate Dynamics*, 42, 1649–1664. https://doi.org/10.1007/s00382-013-1784-y.

Wang, S.-Y., Hipps, L., Chung, O.Y., Gillies, R.R. and Martin, R. (2015) Long-term winter inversion properties in a Mountain Valley of the western U.S. and implications on air quality. *Journal of Applied Meteorology and Climatology*, 54, 2339–2352. https://doi.org/10.1175/JAMC-D-15-0172.1.

Whiteman, C.D. (2000) *Mountain Meteorology: Fundamentals and Applications*. Oxford: Oxford University Press, 376 pp. https://doi.org/10.1093/oso/9780195132717.001.0001.

Whiteman, C.D., Eisenbach, S., Pospichal, B. and Steinacker, R. (2004) Comparison of vertical soundings and sidewall air temperature measurements in a small Alpine Basin. *Journal of Applied Meteorology*, 43, 1635–1647. https://doi.org/10.1175/JAM2168.1.

Whiteman, C.D., Hoch, S.W., Horel, J.D. and Charland, A. (2014) Relationship between particulate air pollution and meteorological variables in Utah's Salt Lake Valley. *Atmospheric Environment*, 94, 742–753. https://doi.org/10.1016/j.atmosenv.2014.06.012.

Whiteman, C.D., Zhong, S., Shaw, W.J., Hubbe, J.M., Bian, X. and Mittelstadt, J. (2001) CAPs in the Columbia basin. *Weather and Forecasting*, 16, 432–447. https://doi.org/10.1175/1520-0434(2001)016<0432:CPITCB>2.0.CO;2.

Williams, A.G., Chambers, S. and Griffiths, A. (2013) Bulk mixing and decoupling of the nocturnal stable boundary layer characterized using a ubiquitous natural tracer. *Boundary Layer Meteorology*, 149, 381–402. https://doi.org/10.1007/s10546-013-9849-3.

Wilson, R., Gutiérrez, D., Gutiérrez, V. and Monserrat, V.J. (2007) An elevational shift in butterfly species richness and composition accompanying recent climate change. *Global Change Biology*, 13, 1873–1887. https://doi.org/10.1111/j.1365-2486.2007.01418.x.

Wolyn, P.G. and McKee, T.B. (1989) Deep stable layers in the intermountain western United States. *Monthly Weather Review*, 117, 461–472. https://doi.org/10.1175/2009WAF2222234.1.

Yao, W. and Zhong, S. (2009) Nocturnal temperature inversions in a small, enclosed basin and their relationship to ambient atmospheric conditions. *Meteorology and Atmospheric Physics*, 103, 195–210. https://doi.org/10.1007/s00703-008-0341-4.

Yu, L., Zhong, S. and Bian, X. (2017) Multi-day valley cold-air pools in the western United States as derived from NARR. *International Journal of Climatology*, 37, 2466–2476. https://doi.org/10.1002/joc.4858.

Zängl, G. (2005a) Dynamical aspects of wintertime cold-air pools in an alpine valley system. *Monthly Weather Review*, 133, 2721–2740. https://doi.org/10.1175/MWR2996.1.

Zängl, G. (2005b) Wintertime cold-air pools in the Bavarian Danube Valley basin: data analysis and idealized numerical simulations. *Journal of Applied Meteorology*, 44, 1950–1971. https://doi.org/10.1175/JAM2321.1.

Zardi, D. and Whiteman, C. (2013) Diurnal Mountain wind systems. Mountain. In: Chow, F., De Wekker, S. and Snyder, B. (Eds.) *Mountain Weather Research and Forecasting*. *Springer Atmospheric Sciences*. Dordrecht: Springer, pp. 35–119. https://doi.org/10.1007/978-94-007-4098-3_2.

Zhong, S., Whiteman, C.D., Bian, X., Shaw, W.J. and Hubbe, J.M. (2001) Meteorological processes affecting the evolution of a wintertime cold air pool in the Columbia Basin. *Monthly Weather Review*, 129, 2600–2613. https://doi.org/10.1175/1520-0493(2001)129<2600:MPATEO>2.0.CO;2.

Zhong, S., Xu, X., Bian, X. and Lu, W. (2011) Climatology of persistent deep stable layers in Utah's Salt Lake Valley, USA. *Advances in Science and Research*, 6, 59–62. https://doi.org/10.5194/asr-6-59-2011.

How to cite this article: Rasilla, D. F., Martilli, A., Allende, F., & Fernández, F. (2023). Long-term evolution of cold air pools over the Madrid basin. *International Journal of Climatology*, *43*(1), 38–56. https://doi.org/10.1002/joc.7700